Journal of Solid State Chemistry **142,** 19–28 (1999)
Article ID jssc.1998.7941, available online at http://www.idealibrary.com on IDEAL®

Lithium Ion Extraction from Orthorhombic $LiMnO_2$ in Ammonium Peroxodisulfate Solutions

Weiping Tang,[1] Hirofumi Kanoh, and Kenta Ooi

Shikoku National Industrial Research Institute, 2217-14, Hayashi-cho, Takamatsu 761-0395, Japan

Received January 12, 1998; in revised form May 18, 1998; accepted June 24, 1998

Well-crystallized orthorhombic $LiMnO_2$ was prepared by a flux method with a (LiCl + LiOH) mixture as the flux. The study of Li^+ extraction from the orthorhombic $LiMnO_2$ was carried out batchwise using a solution containing an oxidizing agent (0.5 mol · dm^{-3} $(NH_4)S_2O_8$). Lithium ions could be extracted from the $LiMnO_2$ without the dissolution of manganese. The time course of Li^+ extraction showed that the Li^+ extraction proceeded in three steps with different extraction rates. Chemical analysis showed that the reaction progressed mainly by a redox mechanism. A structural transformation of orthorhombic $LiMnO_2$ phase to spinel $LiMn_2O_4$ took place at the first and second steps, accompanied by the Li^+ extraction. The structural transformation could be explained well by considering the migration not only of all the lithium ions but also of half of the manganese ions in both oxygen frameworks. The topotactic extraction of Li^+ from $LiMnO_2$ gave a rodlike manganese oxide with a spinel structure. A model of the Li^+ extraction process was proposed as well as a model for the structural transformation from the orthorhombic $LiMnO_2$ to spinel $LiMn_2O_4$. The Li^+ insertion into the Li^+-extracted sample did not proceed in a mixed solution containing 0.1 mol · dm^{-3}LiOH and 0.5 mol · dm^{-3} LiI.

1. INTRODUCTION

The manganese oxide compounds with tunnels or layered structures have attracted attention because of their application as selective adsorbents (1–4), cathode materials for advanced lithium batteries (5–10), and catalysts (11, 12). These compounds have shown different adsorptive properties for metal ions, depending on the size of the tunnel or the interlayer distance. For example, the spinel-type manganese oxide with a $[1 \times 3]$ network shows selective adsorption for lithium ions (1, 2, 13–19), the hollandite type with a $[2 \times 2]$ tunnel for potassium ions (20, 21), the birnessite type with a $[2 \times \infty]$ layer for rubidium ions (22), and the todorokite type with a $[3 \times 3]$ tunnel for cesium ions (23–25). The insertion/extraction reactions of metal ions with these samples progress keeping their tunnel or layered structure. Studies of chemical analyses for manganese oxide samples show that the insertion/extraction reactions of metal ions proceed by two kinds of mechanisms: redox and ionexchange (14, 26–28). The redox type insertion/extraction accompanies the redox reaction of manganese, while the ion exchange reaction proceeds through exchange with lattice protons, without a change in the manganese valence.

Orthorhombic $LiMnO_2$ has a rock salt structure with a distorted cubic close-packed oxygen anion array in which zigzag layers of lithium and manganese cations alternate with one another (29, 30). This material is promising as a cathode material for rechargeable lithium batteries (31–33). Electrochemical studies of Li^+ extraction/insertion with orthorhombic $LiMnO_2$ have indicated that the orthorhombic structure changes to the spinel structure as a result of Li^+ extraction. Such a structural transformation is disadvantageous in a cathode material for a lithium secondary battery. However, the reaction is attractive from a standpoint of inorganic synthesis, because it gives us a new route to prepare a novel material by a so-called soft chemical reaction.

There have been few studies on the mechanism of structural transformation of $LiMnO_2$. The present paper describes the Li^+ extraction reaction with orthorhombic $LiMnO_2$ in the aqueous phase. Well-crystallized orthorhombic $LiMnO_2$ with rodlike shape was prepared by a flux method. The extraction reaction was investigated not by an electrochemical method but by using an $(NH_4)_2S_2O_8$ aqueous solution. Since $(NH_4)_2S_2O_8$ is an oxidizing agent, it depresses the disproportionation of manganese during the extraction reaction in an acidic solution. The use of $K_2S_2O_8$ solution has been studied by Mosbah *et al.* in the Li^+ extraction from $LiMn_2O_4$ spinel (27). They have proposed a redox mechanism for the Li^+ extraction.

2. EXTRACTION PROCESS

The extraction of lithium from $LiMnO_2$ can be classified into two kinds of reactions, ion exchange (Eq. [1]), and redox

[1]To whom correspondence should be addressed. E-mail: tang@sniri.go.jp.

0022-4596/99 $30.00

extraction (Eq. [2]), in analogy to the metal ion extraction reactions with $LiMn_2O_4$ (15, 26) and $Li_{1.33}Mn_{1.67}O_4$ (16).

For ion exchange,

$$LiMn^{III}O_2 + xH^+ \rightarrow Li_{1-x}H_xMn^{III}O_2 + xLi^+ \quad [1]$$

For redox reaction,

$$LiMn^{III}O_2 - xe^- \rightarrow Li_{1-x}Mn^{III}_{1-x}Mn^{IV}_xO_2 + xLi^+. \quad [2]$$

The valence of manganese in the solid phase does not change in the case of ion exchange reaction, whereas it increases from trivalent to tetravalent by the Li^+ extraction in the case of redox reaction. These reactions can be distinguished from one another by analyzing lithium concentration in the solution phase and lattice proton content of the solid before and after the extraction reaction.

The disproportionation of Mn(III) in the solid phase takes place in addition to these reactions in an acidic solution, accompanied by the dissolution of Mn(II) as well as of Li^+,

$$3LiMn^{III}O_2 + 4xH^+ \rightarrow Li_{3-2x}Mn^{III}_{3-2x}Mn^{IV}_xO_{6-2x} + xMn^{2+} + 2xLi^+ + 2xH_2O \quad (0 < x < \tfrac{3}{2}) \quad [3]$$

Since manganese oxide belongs to a one-phase solid solution system (34), the reaction progresses by a surface disproportionation mechanism, as Hunter has proposed for the lithium extraction from $LiMn_2O_4$ spinel (26). This reaction can be distinguished by measuring the Li/Mn ratio in the solution phase. The disproportionation reaction can be depressed by using an appropriate oxidizing agent.

3. EXPERIMENTAL

3.1. Preparation of $LiMnO_2$

A mixture of LiCl (40 g), LiOH (10 g), and γ-MnOOH (5 g) was placed in a high-purity alumina crucible and heated at 650°C for 20 h in a nitrogen atmosphere. The heat-treated sample was immersed in distilled water to dissolve the salt. The $LiMnO_2$ obtained was filtered, washed with water, and dried at 70°C. γ-MnOOH was purchased from Toyo Soda Co., Ltd. (Mn 62.54%, H_2O 0.35%, Fe 0.012%, SiO_2 0.01%, SO_4^{2-} 0.49%, average size 0.85 μm).

3.2. Li^+ Extraction and Insertion

The studies of Li^+ extraction from orthorhombic $LiMnO_2$ were carried out in a 0.5 mol·dm^{-3} $(NH_4)_2S_2O_8$ solution by a batch method at 20°C. $LiMnO_2$ (0.2 g) was added to the $(NH_4)_2S_2O_8$ solution (50 cm^3) and shaken intermittently. After the extraction reaction, the solid was filtered, washed with distilled water, and dried at 70°C.

To make clear the effect of the oxidizing agent $(NH_4)_2S_2O_8$, we studied the Li^+ extraction reaction in a 0.1 mol·dm^{-3} HNO_3 solution under the same conditions as above.

Studies of Li^+ insertion into the Li^+-extracted samples were carried out batchwise using a mixed solution containing 0.1 mol·dm^{-3} LiI and 0.1 mol·dm^{-3} LiOH at 20°C.

3.3. Chemical Analyses

The lithium and manganese concentrations of the supernatant solution were determined by atomic absorption spectrometry. Lithium and manganese contents of $LiMnO_2$ and Li^+-extracted samples were determined after dissolving them in a mixed solution of HCl and H_2O_2. The fraction of Li^+ extraction was calculated as follows:

$$\text{Fraction of } Li^+ \text{ extraction} = \frac{\text{amount of } Li^+ \text{ extracted into solution}}{\text{amount of } Li^+ \text{ in original } LiMnO_2}$$

3.4. Physical Analyses

An X-ray diffraction (XRD) analysis was carried out using a Rigaku type RINT1200 X-ray diffractometer with a graphite monochromator. DTA–TG curves were obtained on a MAC Science thermal analyzer (System 001, TG–DTA 2000) at a heating rate of 10°C/min. SEM observations of the original $LiMnO_2$ and Li^+-extracted samples were carried out on a Hitachi type S-2460N scanning electron microscope.

4. RESULTS AND DISCUSSION

4.1. Characterization of Orthorhombic $LiMnO_2$

XRD analysis indicated that the crystal system was identical to that of orthorhombic $LiMnO_2$ (JCPD card No. 23-0361) with a small portion of Li_2MnO_3 (Fig. 1a). The peak corresponding to the (010) crystal plane was stronger for our sample than those reported by Ohzuku *et al.* (31) or on the JCPD card (No. 23-0361). The lattice constants calculated from the d values of the (120), (010), and (021) crystal planes were 2.82, 5.73, and 4.60 Å for a_0, b_0, and c_0, respectively. A SEM photograph of the $LiMnO_2$ sample shows that it consists of rod crystals of different sizes (Fig. 2).

The DTA–TG curves for the original $LiMnO_2$ are given in Fig. 1b. The curves show an exothermic peak around

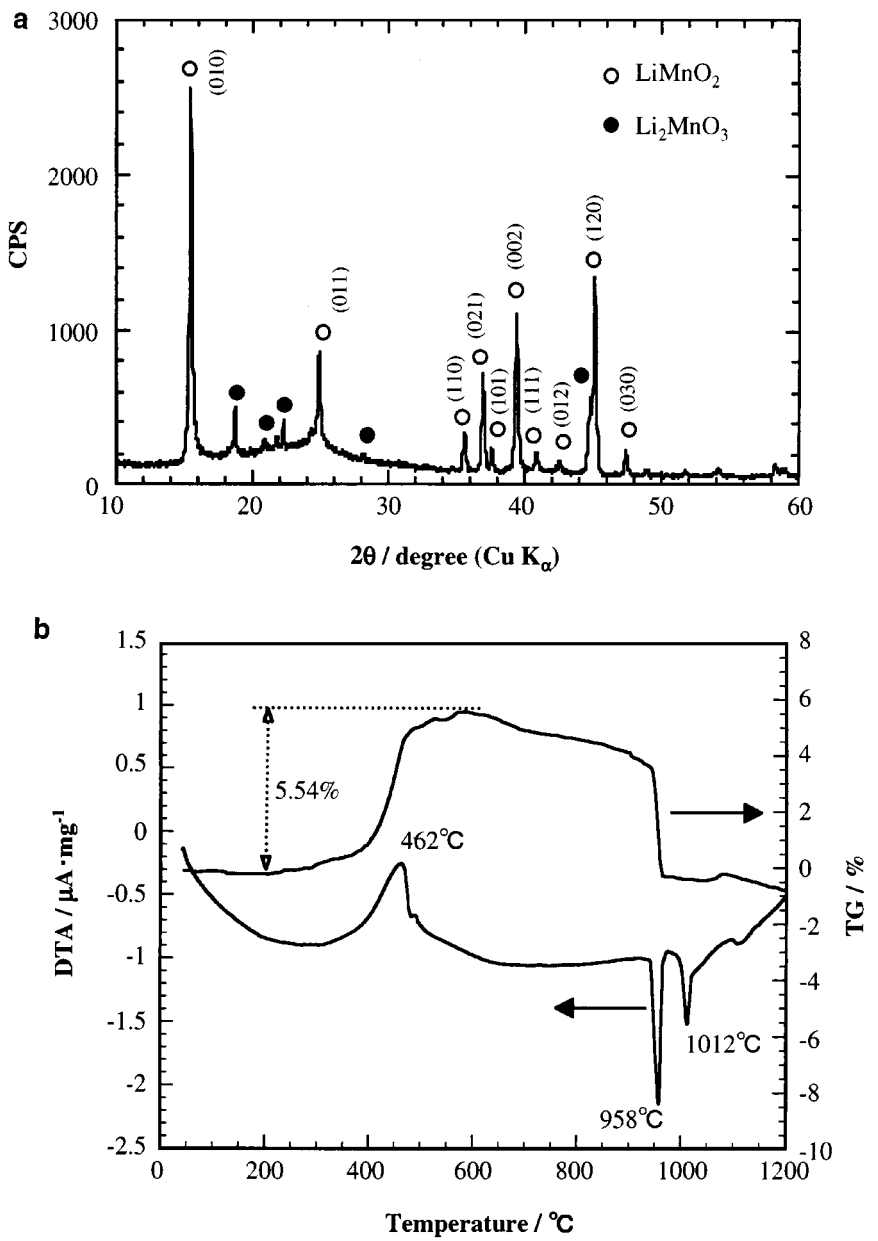

FIG. 1. XRD pattern (a) and TG–DTA curves (b) of original $LiMnO_2$ obtained by a flux method in the MnOOH–LiOH–LiCl system in a N_2 atmosphere at 650°C for 20 h.

462°C accompanied by a weight increment. The XRD pattern of the samples heated at 500°C showed formation of a mixture of the spinel phase ($LiMn_2O_4$) and the monoclinic phase (Li_2MnO_3). This indicates that the exothermic peak around 462°C corresponds to the transformation of orthorhombic $LiMnO_2$ to the mixture of $LiMn_2O_4$ and Li_2MnO_3 accompanied by the absorption of O_2 gas. The reaction can be written as follows:

$$3LiMnO_2 + \tfrac{1}{2}O_2 \rightarrow Li_2MnO_3 + LiMn_2O_4. \quad [4]$$

The weight increment (5.54%) obtained from the TG curve agrees with the theoretical weight increment (5.68%) by reaction [4], indicating that the major compound of the starting material is $LiMnO_2$.

The mole ratio (Li/Mn) of lithium to manganese was 1.10 for the original sample. The chemical formula of the original sample was evaluated as $Li_{1.10}MnO_{2.06}$ on the bases of Li/Mn mole ratio and the weight increment in the TG curve. The formula is close to the theoretical formula of $LiMnO_2$.

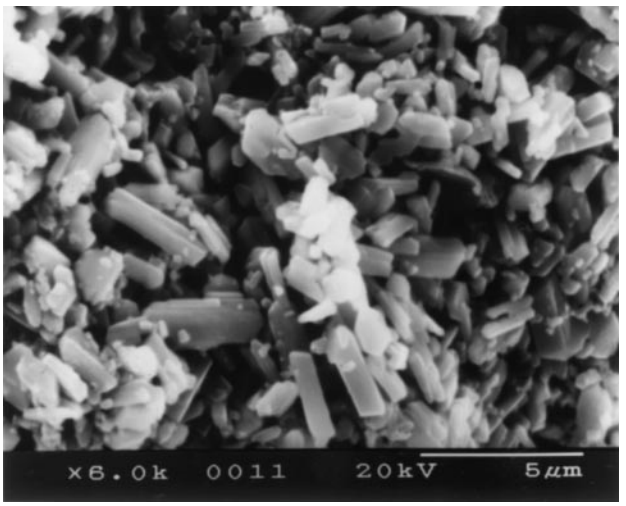

FIG. 2. SEM image of original $LiMnO_2$.

4.2. Li^+ Extraction Reaction in HNO_3 Solutions

Acid treatment of $LiMnO_2$ for 1 day caused a considerable dissolution (4.4 $mmol \cdot g^{-1}$ of sample) of manganese in addition to the extraction (9.6 $mmol \cdot g^{-1}$ of sample) of lithium. The extractability of Li^+ reached 84%. The Li/Mn mole ratio in the solution is 2.2, which is close to the theoretical value (Li/Mn = 2.0) on the basis of the disproportionation reaction of Eq. [3]. The crystal phase of the solid changed from orthorhombic to spinel by the acid treatment. These results indicate that the extraction of lithium proceeds mainly by the surface disproportionation reaction in acidic media.

4.3. Li^+ Extraction Reaction in $(NH_4)_2S_2O_8$ Solution

The extractability of lithium and the dissolution of manganese were studied in a 0.5 $mol \cdot dm^{-3}$ $(NH_4)_2S_2O_8$ solution. The manganese dissolution could not be detected in the supernatant solution by atomic absorption spectrometry (Mn concentration was less than 10^{-6} $mol \cdot dm^{-3}$). This indicates that the disproportionation reaction of Mn(III) is depressed completely by using an oxidizing solution of $(NH_4)_2S_2O_8$, similar to the case of $LiMn_2O_4$ (28). This result indicates that the Li^+ extraction in an $(NH_4)_2S_2O_8$ solution progresses by a mechanism different from that in the HNO_3 solution.

The time course of Li^+ extraction in a 0.5 $mol \cdot dm^{-3}$ $(NH_4)_2S_2O_8$ solution is given in Fig. 3. The fraction of Li^+ extraction and the Li/Mn mole ratio of the solid are plotted against the logarithm of time ($\log t$). The fraction of extracted Li^+ increased rapidly up to about 40% by treatment for 1 day, then increased very slowly up to 4.5 days, but increased again rapidly at $t > 4.5$ days. The plot gives two regions with a straight line at $t \leq 1$ day and $1 < t \leq 4.5$ days with different slopes of 0.048 and 0.009/log d, respectively. We can classify the extraction process into three steps: first ($t \leq 1$ day), second ($1 < t \leq 4.5$ days), and third ($t > 4.5$ days). The Li/Mn mole ratio decreases rapidly to 0.64 with increasing t in the first step but holds an almost constant value of about 0.64 in the second step. It decreases again to 0.44 at $t = 9$ days in the third step. The Li^+ extraction takes place in the first and third steps, but rarely in the second step.

The lattice proton contents were evaluated from the weight loss between 120 and 400°C on the TG curves in a similar manner as the case of spinel type manganese oxide (TG curves are given later) (16). The H^+/Mn mole ratios of the Li^+-extracted sample are given as a function of $\log t$ in Fig. 3. The H^+/Mn mole ratio tends to increase with an increase in the extraction time. However, the H^+/Mn mole ratio is markedly lower than the mole ratio (ΔLi/Mn) of extracted lithium per mole of manganese. This indicates that the ion exchange reaction described by Eq. [1] is a minor reaction in the $(NH_4)S_2O_8$ solution. These chemical analysis results indicate that the major reaction of Li^+ extraction is the redox type (Eq. [2]) in the $(NH_4)S_2O_8$ solution.

4.4. Change in Crystal Phase

X-ray diffraction (XRD) analyses were carried out for the Li^+-extracted samples at different extraction times (Fig. 4). The Li^+-extracted samples in the first step have a crystal system of a mixture of orthorhombic and spinel phases. The peaks corresponding to the (010), (011), and (021) crystal planes of $LiMnO_2$ become weak with the extraction time, accompanied by small shifts to lower 2θ values. The peaks corresponding to the (002) and (120) planes are not observed in the XRD patterns even for samples treated only for 2 h. The peaks corresponding to the spinel phase (111) and (400) planes appear in the XRD pattern of the sample treated for 2 h, and the peak heights increase slightly with time. In the second step, no obvious changes are observed in the strength of the peaks corresponding to the spinel phase, but the peaks corresponding to the orthorhombic $LiMnO_2$ phase become weaker with an increase in t. In the third step, all the peaks can be assigned to those of the spinel phase.

The lattice constants b_0 and c_0 of orthorhombic $LiMnO_2$ in the Li^+-extracted samples were calculated from the d values of the (010) and (012) planes. The a_0 values could not be calculated, since the (120) peak disappeared even by treatment for only 2 h, probably owing to a rapid destruction of a local layered structure. The b_0 value increased from 5.73 to 5.82 Å, whereas the c_0 value decreased from 4.60 to 4.39 Å with an increase in t in the first step. The shrinkage along the c-axis may be advantageous in stabilizing the

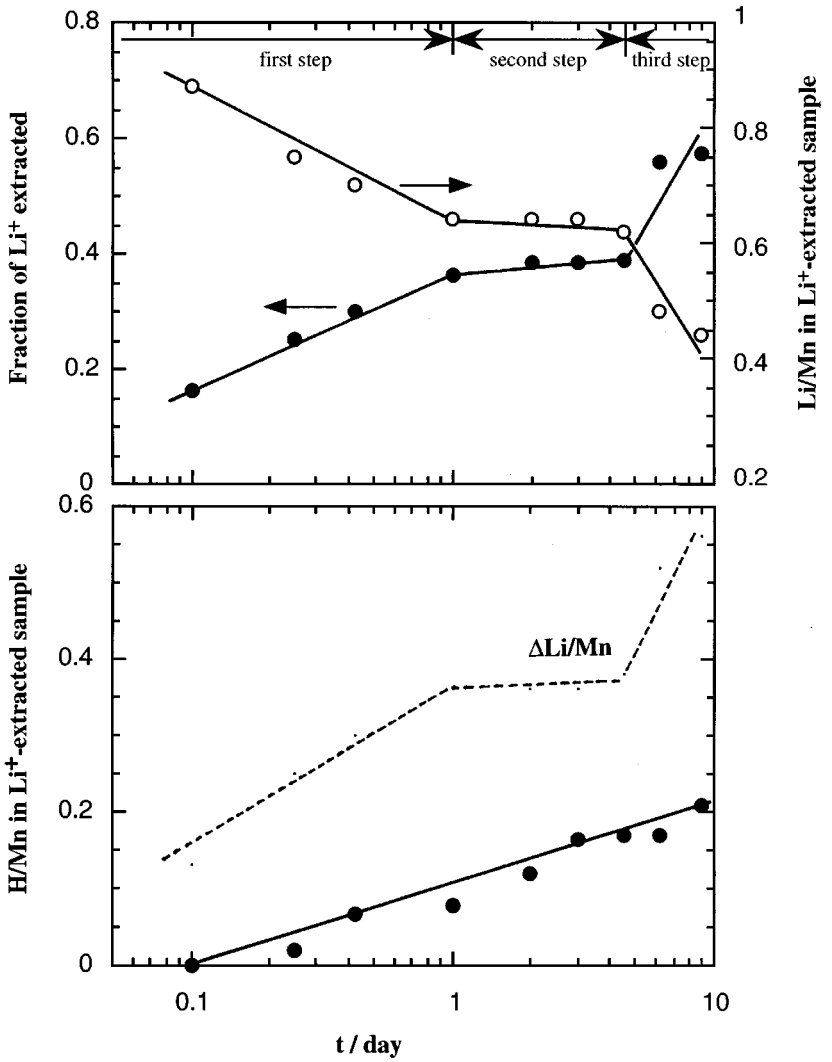

FIG. 3. Changes in the fraction of Li^+ extracted (●) and Li/Mn mole ratio of Li^+-extracted sample (○) with $\log t$ (top). Change in H/Mn mole ratio of Li^+-extracted sample with $\log t$ (bottom). The dotted line describes the amount of extracted lithium per mole of manganese in the solid (ΔLi/Mn).

$[MnO_6]$ octahedron in the Li^+-extracted samples since the $[MnO_6]$ octahedron in $LiMnO_2$ is expanded along the c-axis by Jahn–Teller lattice distortion (35). The lattice constants b_0 and c_0 remained almost constant in the second step.

The peak corresponding to the (400) lattice plane of the spinel type is strong compared to other peaks. A similar feature has been observed in the XRD patterns of samples prepared by electrochemical methods (32, 36), but not in an $LiMn_2O_4$ sample prepared by solid phase reaction methods (16). This peak shows no shift in the first and second steps, whereas it shifts to a higher 2θ direction in the third step. The lattice constant decreases from 8.25 to 8.20 Å in the third step.

These results indicate that Li^+ extraction accompanies the structural transformation in the first and second steps. The structural transformation of orthorhombic $LiMnO_2$ to spinel type is faster in the first step than in the second step. The rate of structural transformation correlates with the decreasing rate of the Li/Mn ratio in the solid phase.

4.5. *Thermal Behavior*

DTA and TG curves of the original $LiMnO_2$ and Li^+-extracted samples at different extraction times are given in Fig. 5. The TG curves show a weight increment around 500°C for the Li^+-extracted samples in the first step, but the DTA curves do not show the exothermic peak, clearly in contrast with the original $LiMnO_2$. The weight increase correlates with the fraction of orthorhombic phase in the solid.

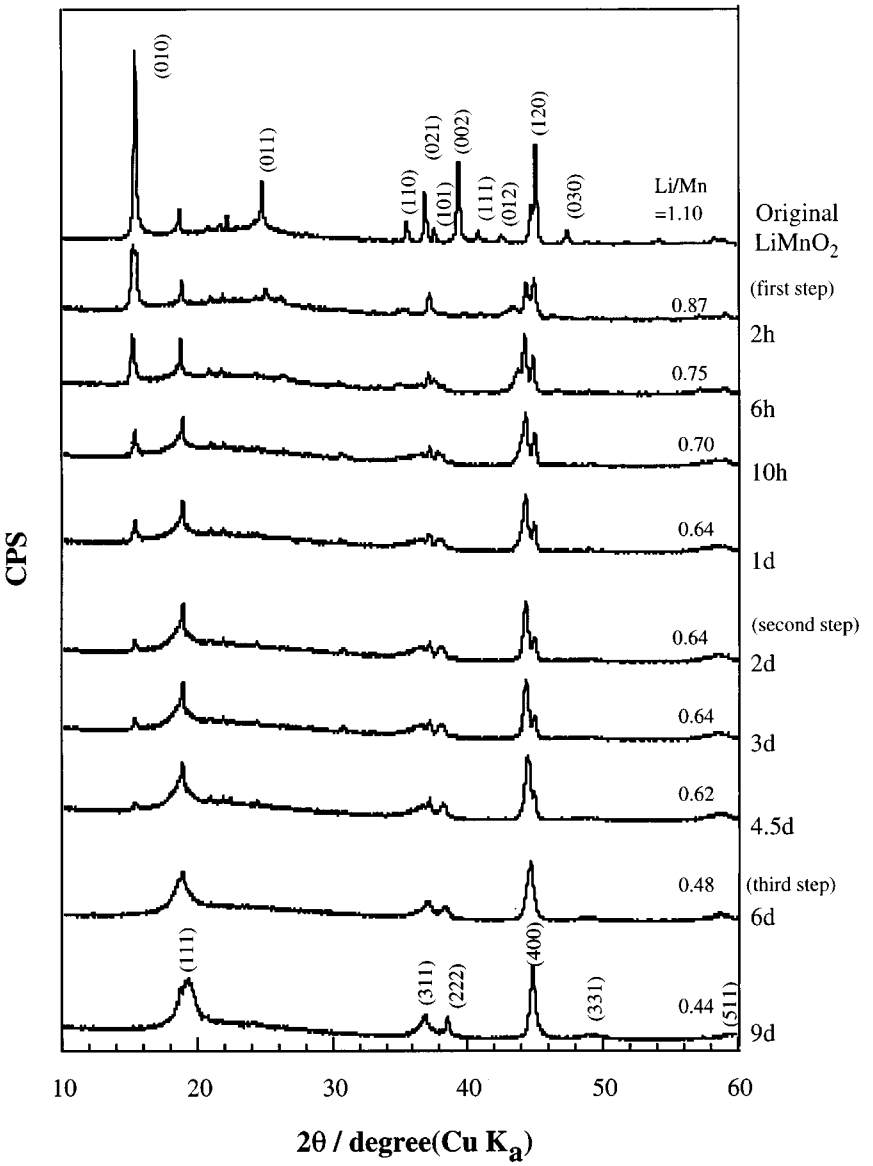

FIG. 4. XRD patterns of the Li^+-extracted samples.

The DTA curves in the second step show exothermic peaks around 200°C; the peak shifts to lower temperatures with an increase in t. These peaks can be assigned to the transformation to a typical spinel phase by XRD analyses; the sample treated at 250°C showed XRD patterns corresponding to a typical $LiMn_2O_4$ phase (JCPD card No. 35-0782), which has the strongest peak at the (111) plane.

The DTA curves of the samples at $t \geq 4.5$ days give an endothermic peak around 240°C with weight loss. These peaks are characterized by the dissipation of water molecules by the condensation of lattice OH groups of the spinel structure (16). They show the presence of Li^+/H^+ ion exchange reaction of the spinel phase in the third step.

4.6. Particle Shape

The SEM photograph of the Li^+-extracted sample at 6 days of treatment shows that the size and shape are similar to those of the original $LiMnO_2$ (Fig. 6). The Li^+ extraction reaction proceeds topotactically without a change of particle shape to give a rodlike manganese oxide with a spinel structure. This is due to the small dissolution of manganese in an $(NH_4)_2S_2O_8$ solution. The rodlike sample has not yet been obtained by conventional synthetic methods. The redox type extraction is useful to prepare a new kind of manganese oxide by a so-called soft chemical route.

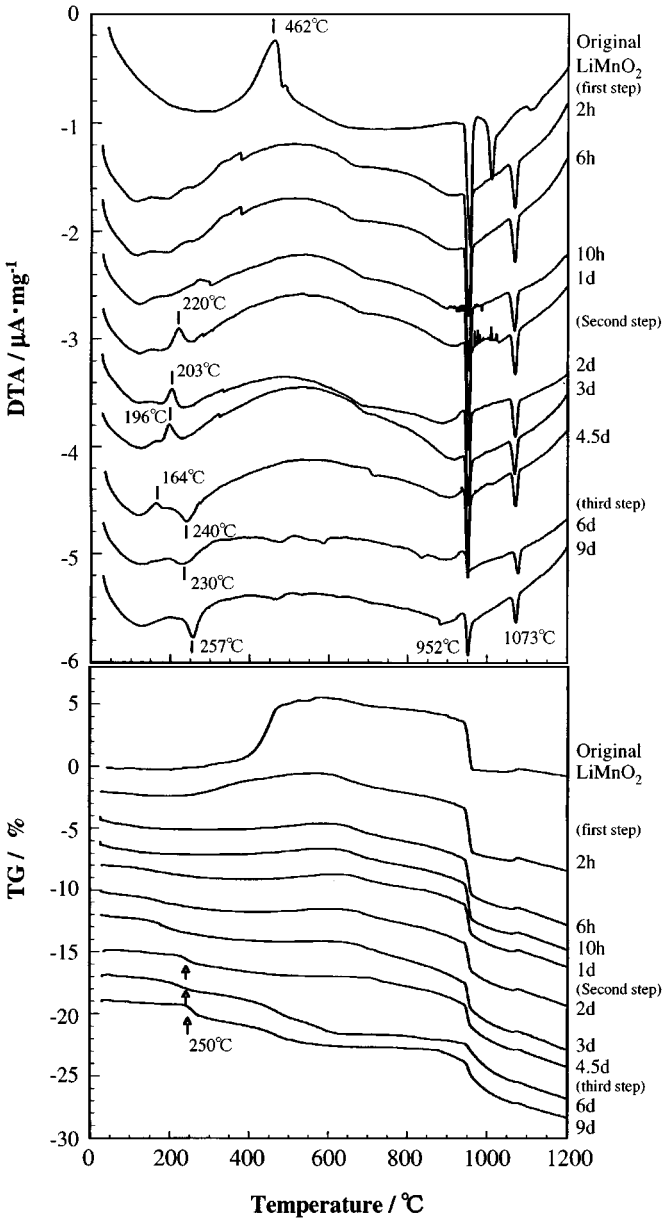

FIG. 5. DTA and TG curves of the Li^+-extracted samples.

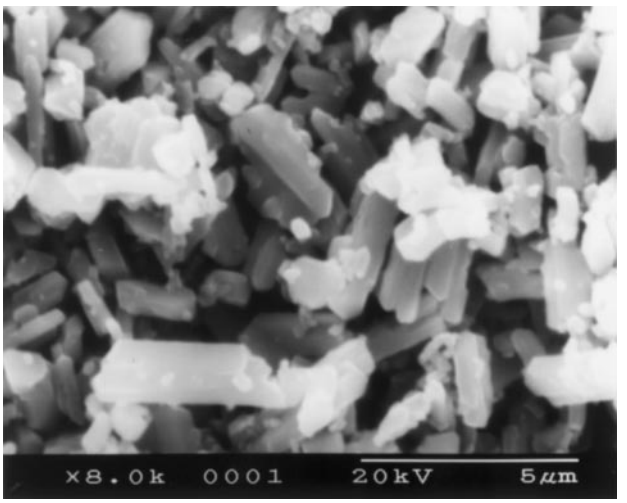

FIG. 6. SEM image of sample treated for 6 days.

4.7. Li^+ Extraction Process

We have proposed two kinds of mechanisms (redox type and ion exchange type) for the Li^+ extraction/insertion with spinel-type lithium manganese oxides in the aqueous phase (14–16, 28). According to the chemical analysis of the extraction reaction, we can propose the Li^+ extraction process, shown schematically in Fig. 7. The Li^+ extraction reaction in the first step proceeds mainly by the redox reaction, since the increase of the H^+/Mn ratio is markedly small, as described before (Fig. 3, bottom). The redox-type extraction is promoted by $(NH_4)_2S_2O_8$. $(NH_4)_2S_2O_8$ is a powerful oxidizing agent in an aqueous solution, since oxygen in $S_2O_8^{2-}$ is in the state of O_2^{2-} instead of O^{2-}. The redox-type Li^+ extraction reaction with orthorhombic $LiMnO_2$ in an $(NH_4)_2S_2O_8$ solution can be described as follows:

$$2LiMn^{III}O_2(s) + xS_2O_8^{2-}(l) \rightarrow 2Li_{1-x}Mn^{III}_{1-x}Mn^{IV}_xO_2(s) + 2xLi^+(l) + 2xSO_4^{2-}(l) \quad [5]$$

The redox-type Li^+ extraction brings about the structural transformation from orthorhombic $LiMnO_2$ to spinel type, in contrast to the case of $LiMn_2O_4$. We have reported previously that the redox-type Li^+ extraction from $LiMn_2O_4$ spinel with a $K_2S_2O_8$ or Br_2 aqueous solution progresses topotactically to give the spinel-type manganese oxide $\square Mn_2O_4$, where $\square$ represents vacant sites at the tetrahedral position (28). The vacant sites are stable enough to keep the spinel structure. In analogy to this reaction, the redox-type Li^+ extraction from $LiMnO_2$ may cause a formation of vacant sites at the "octahedral" position. However, the vacant octahedral sites may be unstable for keeping the orthorhombic structure. As a result, the orthorhombic phase may change to a more stable spinel phase.

The slow Li^+ extraction in the second step can be explained by the influence of the formation of stable $LiMn_2O_4$. We have reported that the solid-state diffusion of Li^+ is a rate-determining process in the Li^+ extraction from $LiMn_2O_4$, and the chemical diffusion coefficient of lithium depends greatly on x in $Li_xMn_2O_4$ (37). The low Li^+ extraction rate in the second step may be caused by the slow Li^+ diffusion in the spinel phase which is formed on the surface of the Li^+-extracted sample. XRD analysis shows the slow transformation from the orthorhombic $LiMnO_2$ phase to

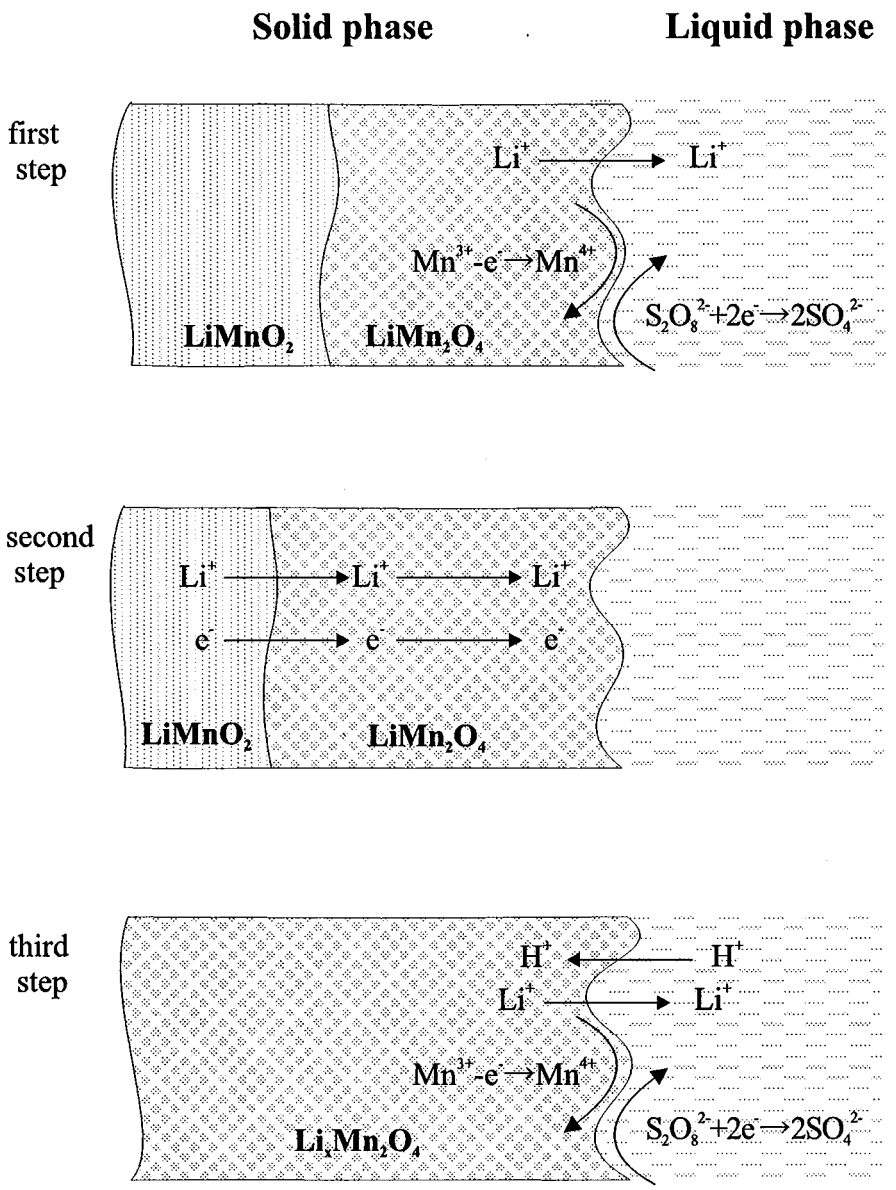

FIG. 7. Schematic representation of Li^+ extraction process.

the spinel phase in the second step, probably caused by the slow Li^+ diffusion in the solid.

The Li^+ extraction reaction in the third step is characteristic of that of spinel-type lithium manganese oxide. The reaction proceeds mainly by the redox mechanism, accompanied by a small portion of ion exchange with H^+. The Li^+ extraction reaction from spinel-type lithium manganese oxide has been studied in detail in the previous papers (16, 26).

4.8. Structural Transformation

The structural transformation of orthorhombic $LiMnO_2$ by Li^+ extraction has been discussed by Gunnow *et al.* in the electrochemical extraction system (32). They have observed the irreversible transformation from the orthorhombic structure to spinel-type $LiMn_2O_4$ by the electrochemical Li^+ extraction. The present transformation resembles their results. The structural transformation can be explained well by comparing the crystal structure of spinel with that of the orthorhombic phase, as illustrated in Fig. 8. The oxygen frameworks are the same for both compounds (Figs. 8a and 8b), assuming that the oxygen position does not change with the Li^+ extraction. The lattice parameter $a_{0,\mathrm{sp}}$ of the spinel structure can be derived from $a_{0,\mathrm{orth}}$ and $b_{0,\mathrm{orth}}$ of orthorhombic $LiMnO_2$ since the direction of the *a*-axis of $LiMn_2O_4$ corresponds to the diagonal lines of a rectangular

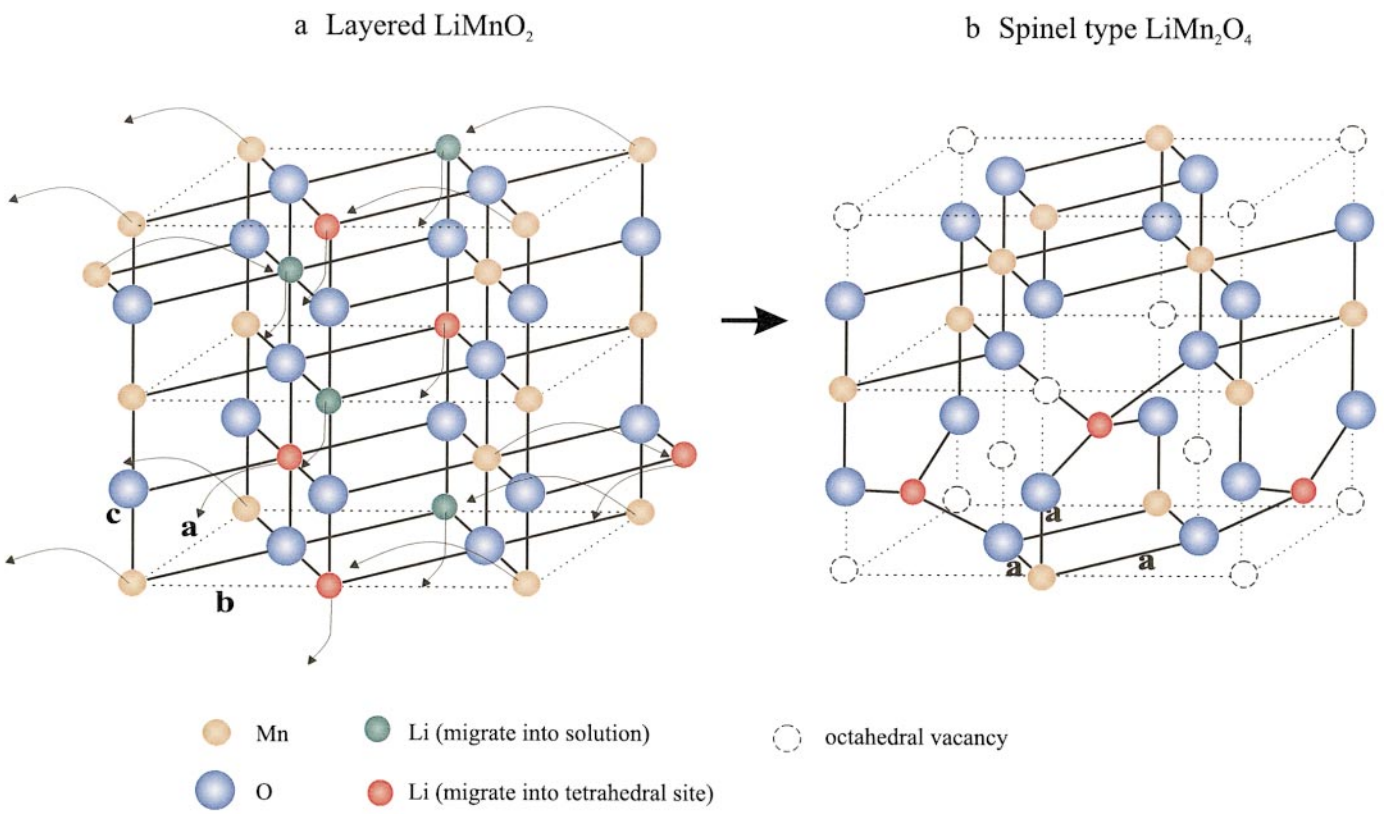

FIG. 8. Schematic representation of the structural transformation of orthorhombic $LiMnO_2$ to spinel-type $LiMn_2O_4$.

cell consisting of $a_{0,\mathrm{orth}}$ and $b_{0,\mathrm{orth}}$ of orthorhombic $LiMnO_2$. The $a_{0,\mathrm{sp}}$ value is calculated as 8.10 Å using $a_{0,\mathrm{orth}} = 2.82$ and $b_{0,\mathrm{orth}} = 5.82$ Å of orthorhombic $LiMnO_2$ in the second step. This value is comparable with the lattice constant $a_{0,\mathrm{sp}}$ (8.25 Å) obtained from XRD patterns in the second step.

The transformation from orthorhombic $LiMnO_2$ to spinel-type $LiMn_2O_4$ needs the migration not only of all lithium ions but also of half of the manganese ions (compare Fig. 8a with 8b). Half of the Li^+ migrates into solution (green balls in Fig. 8a) and the other half into the tetrahedral sites (red balls in Fig. 8a), resulting in the formation of vacant octahedral sites. Then, half of the manganese ions migrate into the vacant octahedral sites. We think that the migration of lithium and manganese ions takes place through neighboring tetrahedral sites as shown in Fig. 8a. The structure of orthorhombic $LiMnO_2$ is characteristic of arraying two Li–O layers with a $[LiO_6]$ octahedron and two Mn–O layers with a $[MnO_6]$ octahedron alternately in the direction of the *b*-axis, as shown in Fig. 8a. The Li^+ extraction leads to a local deviation from electrical neutrality, thus promoting the migration of manganese ions. In addition, the distorted $[MnO_6]$ array along the *c*-axis in the orthorhombic $LiMnO_2$ makes the migration of lithium and manganese ions easy.

4.9. Insertion of Li^+ in an LiI + LiOH solution

Li^+ insertion into the Li^+-extracted samples was studied in a mixed solution containing 0.1 $mol \cdot dm^{-3}$ LiOH and 0.1 $mol \cdot dm^{-3}$ LiI. Two kinds of Li^+-extracted samples with Li/Mn mole ratios of 0.64 and 0.48 were used. The Li^+ concentration in the supernatant solutions did not change after the Li^+ insertion experiment. Also, no obvious changes were observed between the XRD patterns of the samples before and after the Li^+ insertion experiment. These results indicate that the redox-type Li^+ extraction from $LiMnO_2$ is irreversible in the aqueous phase.

5. CONCLUSIONS

Li^+ can be extracted from orthorhombic $LiMnO_2$ without a dissolution of manganese by treating it in an oxidizing agent $(NH_4)_2S_2O_8$ solution. The reaction proceeds mainly by the redox mechanism, keeping the original particle shape, while it is accompanied by a structural transformation from the orthorhombic to the spinel phase. The structural transformation of the orthorhombic phase $LiMnO_2$ to the spinel phase $LiMn_2O_4$ can be explained by the migration not only of lithium but also of manganese ions throughout the oxygen framework. The redox-type extraction is

useful to prepare a new kind of manganese oxide by a soft chemical reaction.

REFERENCES

1. X. M. Shen, and A. Clearfield, *J. Solid State Chem.* **64,** 270 (1986).
2. V. V. Vol'khin, G. V. Leont'eva, and S. A. Onolin, *Neorg. Mater.* **6,** 1041 (1973).
3. K. Ooi, Y. Miyai, and S. Katoh, *Sep. Sci. Technol.* **22,** 1779 (1987).
4. Q. Feng, H. Kanoh, Y. Miyai, and K. Ooi, *in* "Proceedings of the International Conference on Ion Exchange," Takamatsu, 1995, p. 141.
5. M. M. Thackery, W. I. F. David, P. G. Bruce, and J. B. Goodenough, *Mater. Res. Bull.* **18,** 461 (1983).
6. M. M. Thackeray, P. J. Johnson, L. A. D. Piccioto, W. I. F. David, and J. B. Goodenough, *Mater. Res. Bull.* **19,** 179 (1984).
7. T. Ohzuku, J. Kato, K. Swai, and T. Hirai, *J. Electrochem. Soc.* **138,** 2556 (1991).
8. M. H. Rossouw, D. C. Liles, and M. M. Thackeray, *Mater. Res. Bull.* **27,** 221 (1992).
9. J. M. Tarascon E. Wang, and F. K. Shokoohi, *J. Electrochem. Soc.* **138,** 2859 (1991).
10. R. N. De Guzman, Y. F. Shen, B. R. Shaw, S. L. Suib, and C. L. O'Young, *Chem. Mater.* **5,** 1395 (1993).
11. M. N. Richard, E. W. Fuller, and J. R. Dahn, *Solid State Ionics* **73,** 81 (1994).
12. M. F. Ryan, A. Fiedler, D. Schroder, and H. Schwarz, *J. Am. Chem. Soc.* **117,** 2033 (1995).
13. K. Ooi, Y. Miyai, S. Katoh, H. Maeda, and M. Abe, *Langmuir* **5,** 150 (1989).
14. K. Ooi, Y. Miyai, and J. Sakakihara, *Langmuir* **7,** 1167 (1991).
15. H. Kanoh, K. Ooi, Y. Miyai, and S. Katoh, *Langmuir* **7,** 1841 (1991).
16. Q. Feng, Y. Miyai, H. Kanoh, and K. Ooi, *Langmuir* **8,** 1861 (1992).
17. H. Kanoh, Q. Feng, Y. Miyai, and K. Ooi, *J. Electrochem. Soc.* **140**, 3162 (1993).
18. G. R. Burns, C. Kane, and N. Sahasrabudha, *in* "New Developments in Ion Exchange" (M. Abe, T. Kataoka, and T. Suzuki, Eds.), p. 523. Kodansha and Elsevier, Tokyo, Amsterdam, 1991.
19. B. Ammundsen, D. J. Jones, J. Roziere, and G. Burns, *Chem. Mater.* **8,** 2799 (1996).
20. M. Tsuji and S. Komarneni, *J. Mater. Res.* **8,** 611 (1993).
21. Q. Feng, H. Kanoh, Y. Miyai, and K. Ooi, *Chem. Mater.* **7,** 148 (1995).
22. Q. Feng, H. Kanoh, Y. Miyai, and K. Ooi, *Chem. Mater.* **7,** 1226 (1995).
23. Q. Feng, H. Kanoh, Y. Miyai, and K. Ooi, *Chem. Mater.* **7,** 1722 (1995).
24. Y. F. Shen, R. P. Zerger, S. L. Suib, L. McCurdy, D. I. Potter, and C. L. O'Young, *J. Chem. Soc., Chem. Commun.* **17,** 1213 (1992).
25. Y. F. Shen, R. P. Zerger, R. N. DeGuzman, S. L. Suib, L. McCurdy, D. I. Potter, and C. L. O'Young, *Science* **26,** 511 (1993).
26. J. C. Hunter, *J. Solid State Chem.* **39,** 142 (1981).
27. A. Mosbah, A. Verbaere, and M. Tournoux, *Mater. Res. Bull.* **18,** 1375 (1983).
28. K. Ooi, Y. Miyai, S. Katoh, H. Maeda, and M. Abe, *Chem. Lett.* 989 (1988).
29. G. Dittrich and R. Hoppe, *Z. Anorg. Allg. Chem.* **365,** 337 (1969).
30. F. Leroux, D. Guyomard, and Y. Piffard, *Solid State Ionics* **80,** 299 (1995).
31. T. Ohzuku, A. Ueda, and T. Hirai, *Chem. Express* **2,** 193 (1992).
32. R. J. Gunnow, D. C. Liles, and M. M. Thackeray, *Mater. Res. Bull.* **28,** 1249 (1993).
33. M. Tabuchi, K. Ado, C. Masquelier, I. Matsubara, H. Sakaebe, H. Kageyama, H. Kobayashi, R. Kanno, and O. Nakamura, *Solid State Ionics* **89,** 53 (1996).
34. A. Kozawa and R. A. Powers, *J. Electrochem. Soc.* **113,** 870 (1966).
35. G. Pistoia, A. Antonini, and D. Zane, D. *Solid State Ionics* **78,** 115 (1995).
36. J. N. Reimers, E. W. Fuller, E. Rossen, and J. R. Dahn, *J. Electrochem. Soc.* **140,** 3396 (1993).
37. H. Kanoh, Q. Feng, T. Hirotsu, and K. Ooi, *J. Electrochem. Soc.* **143,** 2610 (1996).